NASA/TP—2010–216434

Simplification of Fatigue Test Requirements for Damage Tolerance of Composite Interstage Launch Vehicle Hardware

A.T. Nettles, A.J. Hodge, and J.R. Jackson
Marshall Space Flight Center, Marshall Space Flight Center, Alabama

June 2010

The NASA STI Program…in Profile

Since its founding, NASA has been dedicated to the advancement of aeronautics and space science. The NASA Scientific and Technical Information (STI) Program Office plays a key part in helping NASA maintain this important role.

The NASA STI Program Office is operated by Langley Research Center, the lead center for NASA's scientific and technical information. The NASA STI Program Office provides access to the NASA STI Database, the largest collection of aeronautical and space science STI in the world. The Program Office is also NASA's institutional mechanism for disseminating the results of its research and development activities. These results are published by NASA in the NASA STI Report Series, which includes the following report types:

- TECHNICAL PUBLICATION. Reports of completed research or a major significant phase of research that present the results of NASA programs and include extensive data or theoretical analysis. Includes compilations of significant scientific and technical data and information deemed to be of continuing reference value. NASA's counterpart of peer-reviewed formal professional papers but has less stringent limitations on manuscript length and extent of graphic presentations.

- TECHNICAL MEMORANDUM. Scientific and technical findings that are preliminary or of specialized interest, e.g., quick release reports, working papers, and bibliographies that contain minimal annotation. Does not contain extensive analysis.

- CONTRACTOR REPORT. Scientific and technical findings by NASA-sponsored contractors and grantees.

- CONFERENCE PUBLICATION. Collected papers from scientific and technical conferences, symposia, seminars, or other meetings sponsored or cosponsored by NASA.

- SPECIAL PUBLICATION. Scientific, technical, or historical information from NASA programs, projects, and mission, often concerned with subjects having substantial public interest.

- TECHNICAL TRANSLATION. English-language translations of foreign scientific and technical material pertinent to NASA's mission.

Specialized services that complement the STI Program Office's diverse offerings include creating custom thesauri, building customized databases, organizing and publishing research results…even providing videos.

For more information about the NASA STI Program Office, see the following:

- Access the NASA STI program home page at <http://www.sti.nasa.gov>

- E-mail your question via the Internet to <help@sti.nasa.gov>

- Fax your question to the NASA STI Help Desk at 443–757–5803

- Phone the NASA STI Help Desk at 443–757–5802

- Write to:
  NASA STI Help Desk
  NASA Center for AeroSpace Information
  7115 Standard Drive
  Hanover, MD 21076–1320

NASA/TP—2010–216434

Simplification of Fatigue Test Requirements for Damage Tolerance of Composite Interstage Launch Vehicle Hardware

A.T. Nettles, A.J. Hodge, and J.R. Jackson
Marshall Space Flight Center, Marshall Space Flight Center, Alabama

National Aeronautics and
Space Administration

Marshall Space Flight Center • MSFC, Alabama 35812

June 2010

Acknowledgments

This work was supported by NASA under the auspices of the Upper Stage Program Office at Marshall Space Flight Center.

Available from:

NASA Center for AeroSpace Information
7115 Standard Drive
Hanover, MD 21076–1320
443–757–5802

This report is also available in electronic form at
<https://www2.sti.nasa.gov>

TABLE OF CONTENTS

LIST OF FIGURES

LIST OF TABLES

LIST OF ACRONYMS AND SYMBOLS

BVID	barely visible impact damage
CAI	compression after impact
IRT	infrared thermography
LL	limit load
MSFC	Marshall Space Flight Center
NDE	nondestructive evaluation
S-N	stress versus number of cycles to failure curve
TP	Technical Publication
UL	ultimate load

NOMENCLATURE

n	design load limit to flight
σ_{AVG}	breaking stress
σ_{LL}	limit load stress
σ_{UL}	ultimate load stress

TECHNICAL PUBLICATION

SIMPLIFICATION OF FATIGUE TEST REQUIREMENTS FOR DAMAGE TOLERANCE OF COMPOSITE INTERSTAGE LAUNCH VEHICLE HARDWARE

1. INTRODUCTION

One of the fracture control requirements for composite hardware on manned launch vehicles is that damage will not propagate and result in failure. MSFC–RQMT–3479, Fracture Control Requirements for Composite and Bonded Vehicle and Payload Structures, requires coupon level curves to be generated for (a) residual compression strength as a function of damage size for a multiple number of load cycles, (b) life curves for multiple damage sizes, and (c) threshold compression strain for multiple damage sizes.[1] Examples of these three types of curves are shown in figure 1.

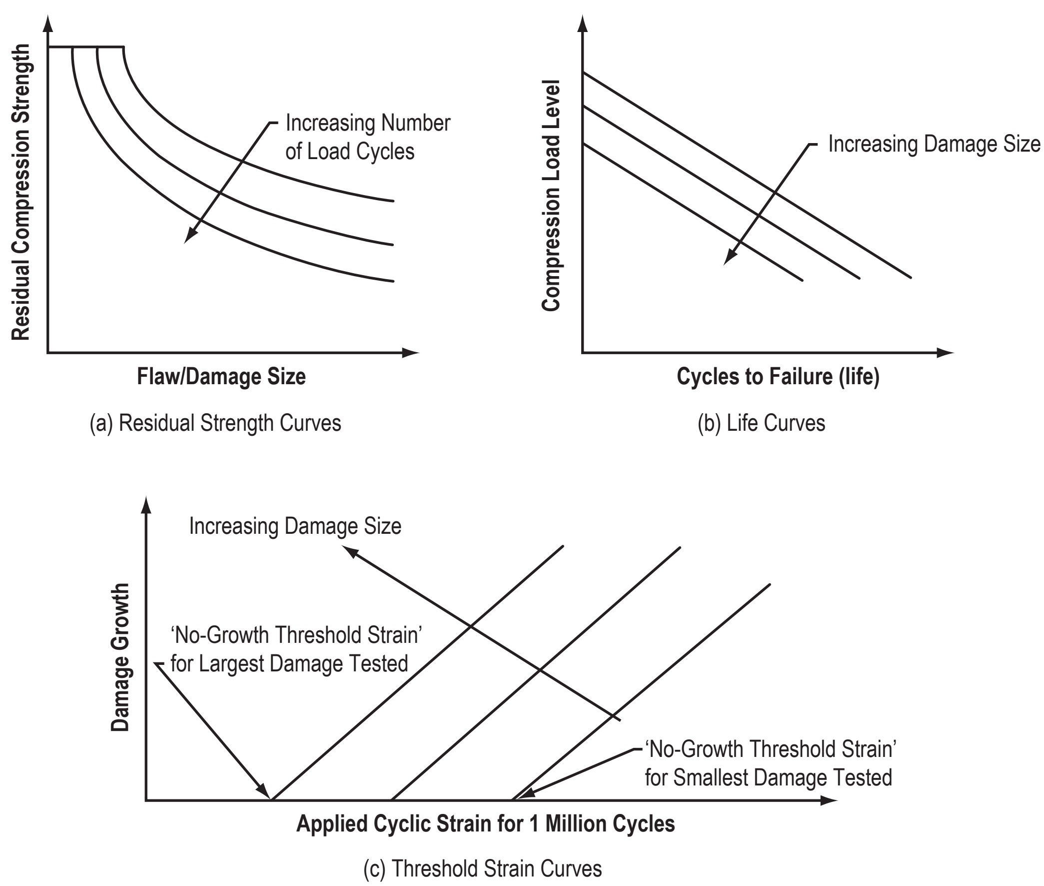

Figure 1. Damage tolerant coupon test schematics.[1]

Figure 1(a) is based on the assumption that fatigue loading will decrease the residual compression strength of a composite laminate for a given damage size. For example, the upper curve may represent the static case most often published in literature. The curves below that are plots of compression strength versus damage size after the specimens have been fatigue loaded and are assumed to be lower than the static case (i.e., it is assumed fatigue will be detrimental to the compression strength of a laminate with a flaw).

Figure 1(b) illustrates the typical stress versus number of cycles to failure (S-N) curve found in the literature for metallic materials in tension. These curves are based on the assumption that, as the cyclic compressive load increases, the number of cycles to failure will decrease and the degradation rate is the same regardless of damage size.

Figure 1(c) determines the compressive strain level at which damage will not grow after 1 million cycles. The value of 1 million is arbitrarily chosen as runout, after which the component is expected to be retired from service. This figure assumes a very long lifetime of the part (1 million cycles at a significant strain). Furthermore, this figure assumes that damage will grow and that growth can be measured with some sort of nondestructive technique before catastrophic failure.

To generate these curves, a large number of specimens needs to be tested under fatigue, which is time consuming. Since composite laminates behave differently in fatigue than metallic structures, it is worth noting the differences to examine if the construction of these curves can be simplified, thus reducing testing time and costs. In addition, specifics related to launch vehicles (as opposed to aircraft) will be noted so that they can be used to further simplify obtaining the necessary information to design a damage-tolerant launch vehicle structure.

2. BACKGROUND

The effects of cyclic loading on the structure's material and the life cycle of the structure must be taken into account when the structure is being assessed for fatigue. Due to shorter operational times, expendable rocket components will experience fewer cyclic loads than fixed wing aircraft components, and fixed wing aircraft will experience fewer cycles than rotating hardware on rotorcraft. This will determine when runout is considered to have occurred and will be discussed more in section 2.2. The next section presents a review of the compressive cyclic loading aspects from past studies in the open literature and what may be expected in this Technical Publication (TP).

Since the terms 'breaking,' 'ultimate,' and 'limit' loads are used differently according to industry practice, the terms used in the remainder of this TP will be defined below. The terms 'stress' and 'strength,' as used in this study, will also be defined.

Breaking load is simply the load at which catastrophic failure of the laminate occurs. For a test series with 15 specimens, there will be 15 unique and distinct breaking loads.

Average breaking load is the statistic used as an estimator for population mean and is equal to the sum of individual breaking loads divided by the number of individual loads. The confidence band on the estimate of mean improves with increasing replications and reducing variance. The average breaking load can also be referred to as 'expected' breaking load.

Ultimate load (UL) is a statistically based value above which a certain percentage of specimens are expected to survive with a given confidence level. Typically, a 'B-Basis value' means a load at which there is a 95% confidence level that at least 90% of the specimens will survive. This value is at the lower tail of the breaking load probability distribution. An 'A-Basis value' means a load at which there is a 95% confidence level that at least 99% of the specimens will survive.

Limit load (LL) is the maximum load expected on a structure during its design life. In order for a structure to have a positive margin of safety, the LL must be less than the UL divided by a factor of safety. For the aerospace components mentioned in this study, the factor of safety is 1.4. Thus, LL must not exceed 71.4% of the UL.

Stress is load divided by the initial cross-sectional area of a specimen. The cross-sectional area of all specimens in this study was the same, so transforming between load and stress is straightforward. The symbols for average breaking stress, ultimate stress, and limit stress are σ_{AVG}, σ_{UL}, and σ_{LL}, respectively.

In this TP, 'strength' is the σ_{AVG} of a specimen and, more specifically, compression after impact (CAI) strength is the compressive σ_{AVG} of a specimen that has experienced a foreign object impact event.

2.1 Effects of Fatigue

A review of the literature was performed on previous work regarding the detection, measurement, and consequences of damage growth due to compressive fatigue loading. Tension fatigue and/or the use of artificially induced delaminations, rather than impact damage, where not considered in order to keep the literature review as close to the planned experimental part of this study as possible.

Table 1 summarizes the pertinent results from a variety of compression-fatigue-after-impact test programs conducted in the past. The majority of past studies examined specimens with barely visible impact damage (BVID). Most components are required and designed to carry the UL with BVID. Therefore, past studies have set BVID as the threshold for allowable damage size. Table 1 presents compression load as a percentage of the average (or expected) breaking load of a sample with the same level of damage so a direct comparison between studies could be made. In some cases, this percentage had to be calculated from the data since compression fatigue amplitude as a percentage of average strength was not always explicitly given and is detailed in the footnotes below the table. The cycles to failure column presents the highest and lowest number of cycles to failure, which typically corresponds to the lowest and highest loads in the previous column. It was of interest to see if other experimental programs found damage growth (using any nondestructive technique), so a 'growth detected' column was added.

Since two of the studies used variable amplitude fatigue spectrums, the maximum amplitude in the spectrum is presented. The corresponding cycles are the numbers of cycles to this maximum load, while no other load excursions are counted. The results are presented as the number of 'programs' that survived. Each program had 200 excursions to the maximum amplitude load and the necessary conversions were made to fit the data into table 1.

Only three studies in table 1 published data for compression stress amplitudes <60% of the predicted static CAI stress. In these three studies, the specimens all experienced no deleterious effects when fatigued <60% of the static strength value. This is indicative of the good fatigue properties of composites in which the fibers have a crack retardation effect for the multitude of matrix cracks that form during fatigue as demonstrated by Reifsnider[19,20] and Kunz.[21] One of the earliest realizations noted over two decades ago was that ≈60% of static CAI failure stress is the 'lower boundary of a fatigue failure regime.'[16] The lower bound of 60% of static CAI failure stress was also suggested in reference 8, which found that, in addition to this lower bound, compressive stress ranges (difference between consecutive stress levels) on the order of 20% could also be eliminated from the fatigue load spectrum since they have no deleterious effects. Also of note are the results of fatigue data published in which damage initiated from the free edge of impact damaged test specimens[22] or cutouts[23] before any growth was seen in the impact damage area, indicating that free edges may be more of a fatigue concern than impact damage.

When examined on a basis of damage severity, the fatigue life of laminates tends to improve (i.e., the S-N curve gets flatter as more damage is induced).[2,13,15] The static compressive strength drops with increasing damage but the effects of fatigue are diminished. This leads to the conclusion that the undamaged case will be the most conservative when examining the fatigue life of expendable structures in compression.

Table 1. Summary of compression fatigue after impact data from the open literature.

Type Specimen	Compression Amplitude Range*	Cycles to Failure	Compression Strength if Survived Fatigue*	Growth Detected
48-ply AS4/3501-6[2]	88–97	496,509–533	N/A	No
8-ply sandwich AS4/3501-6[2]	73–112**	∞***–5 (∞ = 60,000)	≈109†	6 of 17
48- and 42-ply AS4/3501-6 (blunt impact)[3]	71–81	∞ (∞ = 1 million)	N/A	1 of 4
48- and 42-ply AS4/3501-6 (penetration impact)[3]	64–73	∞ (∞ = 1 million)	N/A	4 of 4
48-ply IM7/HTAC (thermoplastic)[4]	60–78	2 million–200	N/A	No
48-ply IM7/BMI[4]	71–90	1.5 million–1,000	N/A	Yes
16-ply IM7/PEEK[5]	60	∞ (∞ = 1 million)	≈100	No
16-ply IM7/epoxy[5]	60	∞ (∞ = 1 million)	≈110	3 of 17
T50/934 6-ply tubes[6]	75	∞–8,931 (∞ = 1 million)	100	No
48-ply IM7/8551-7[7]	68–75	301,000–7,050	N/A	N/A
32-ply AS4/3501-6[8]	30–80	∞–136 (∞ = 1 million)	105	Yes above 70%
21-ply T300/914[9]	67–97	781,321–2	N/A	Yes near failure
16-ply AS4/8552[10]	75–85	∞–≈1,000 (∞ = 1 million)	N/A	Yes at 85%
4-ply sandwich carbon/epoxy fabric[11]	20–90	∞–≈2 (∞ = 150,000)	70–115	N/A
48-ply HTA/6376[12]	60–90	∞–120 (∞ = 1 million)	N/A	Yes near failure
24-ply UT500/QU135-197A[13]	79–98	≈5,000–150	N/A	Yes
32-ply AS4/PEEK[13]	66–98	≈900,000–60	N/A	Very Little
2-mm-thick T300/vinylester fabric[14]	60–80	≈1 million–300	N/A	No
16-ply carbon/epoxy5[‡,15]	62–80	∞–9,000 (∞ = 1 million)	N/A	No
56-ply XAS/914C[16]	88§	107,600–6,800	N/A	Yes
56-ply XAS/914C[17]	88§	30,000–600	80–89	Yes
32-ply IM7/3501-6[18]	74–84	∞ –33,500 (∞ = 1 million)	121–134	No
32-ply IM7/8551-7[18]	33–78	∞ –4,330 (∞ = 1 million)	90–109	No

*Values given as a percentage of the average static CAI strength.
**Values can be >100% due to scatter in the static data not being accounted for.
***∞ implies runout.
†Growth detected on all samples tested post fatigue.
‡Details on material not given.
§Maximum value of spectrum loading.

In the only study that saw any damage growth at a load value <60% of the static strength value, the specimens were first preloaded in a block loading at high fatigue amplitude >60% in order to initiate damage growth.[22] However, according to reference 1, loading was on a 'failed' specimen.

Another interesting result seen in table 1 is that the strength after fatigue was the same or higher than the expected static CAI strength in most of the studies in which the residual compression strength of fatigued specimens were tested. This was most pronounced in reference 18 for a brittle matrix composite. The authors in this study did not conclude a physics based reason for this; however, they did mention that such results were found for tension testing of open hole laminates.[24,25] These strength improvements due to fatigue were seen even when damage growth had occurred.

For the studies in which damage growth did occur, the growth was seen to occur near the end of the load spectrum with damage rapidly increasing as failure was reached. This indicates that determination of a 'no-growth' threshold strain will be difficult to determine. A thorough treatment of the evolution of impact damage growth is given by Chen et al. in which the damage growth is seen to occur in three distinct phases as shown in figure 2.[10] By utilizing real-time acoustography, more detailed information about the damage size could be made without unloading and reloading specimens. For constant amplitude fatigue loading at amplitude 75% or less of average CAI strength, no growth occurred before runout, which was considered 1 million cycles. For specimens that did demonstrate damage growth (80% and 85% of average CAI strength) a three-phase growth pattern was observed. Phase 1 shows rapid growth before slowing dramatically. During this period, the increase in impact damage size is due to a change in shape of the impact damage in which the planar area of damage simply achieves smoother edges.

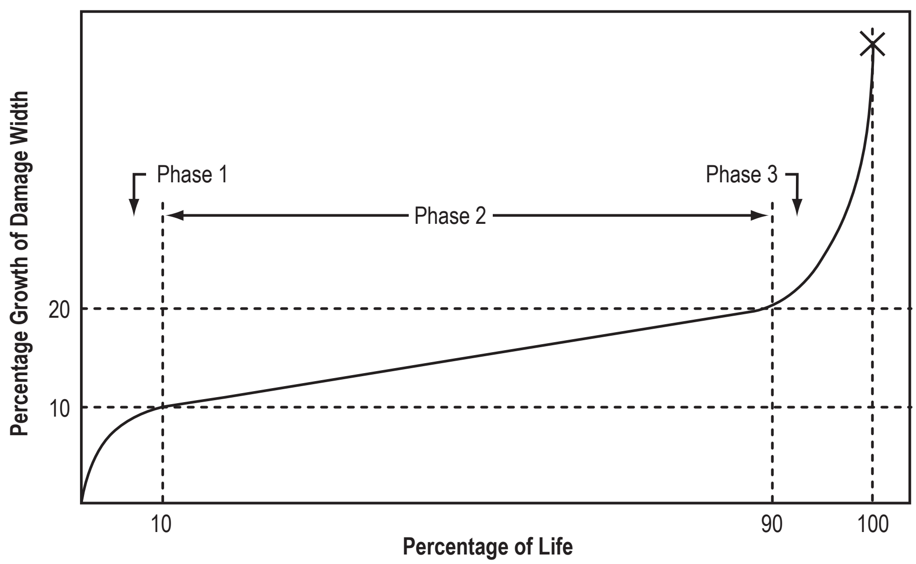

Figure 2. Schematic of impact damage growth showing three phases during fatigue testing.

Phase 2 consists of the vast majority of the life of the specimen and is a period of very slow growth until phase 3 is reached. At this point, the growth of the impact damage area becomes rapid near the end of the life of the specimen. Phase 3 growth, which is easier to detect using more conventional nondestructive evaluation (NDE) techniques, has been seen in other studies that do not have the fidelity to observe the phase 2 slow growth.[8,9,16] A study that used digital speckle photometry also showed three regions of damage growth like that illustrated in figure 2.[12] These results indicate that determination of a 'no-growth' threshold strain is more difficult to define than it is for metals. 'No detrimental growth' is a more accurate term for composites since rounding (the formation of smoother areas of the planar area of damage) of the damage area can be beneficial to residual compression strength of impact damaged laminates.[2,5,8,11,18]

Reference 1 does not mention tension or in-plane shear after impact for launch vehicle hardware that is driven by either of these two types of loading. It has been shown that static compression after impact strength degrades more than static tension after impact strength for a given level of damage severity;[26–31] therefore, compression of a damaged laminate will be of more criticality than tension of a laminate with the same level of impact damage. The tensile aspects of a structure designed primarily for tensile loads, such as a rocket motor case, should be considered since tensile and compressive failure modes are different and independent in composite laminates.[32]

2.2 Load Spectrum

The number of cycles, amplitude, and R-ratio at which to test specimens after impact will obviously depend upon the application and hardware in question. Virtually all of the current knowledge and literature on this subject is from the aircraft and rotorcraft industry. Conservative measures are used because the manufacturers of airplanes and helicopters do not know the specific load profile of each flight or how long one flight may last. Since expendable launch vehicles have a value of one flight/life, requiring four lifetimes to account for material variability and a given number of excursions to design limit load per flight (n) results in $4n$ cycles at LL to demonstrate fatigue life. Since the part is not to be used again, phase 2 nondetrimental damage growth is of no practical consequence.

The order of applied loads is not critical for spectrum fatigue loading of composites.[8,16,17] Thus, to facilitate fatigue testing, the highest loads are tested first to accelerate the testing process. If the highest blocks of loads do not cause degradation or failure, the lower loads are removed from the spectrum.[33]

As an example, the load spectrum for the composite interstage for the Ares I launch vehicle is shown in figure 3. As can be seen, the structure will experience one cycle at LL and two cycles at a value >50% of LL, thus simplifying the fatigue spectrum as shown in figure 4.

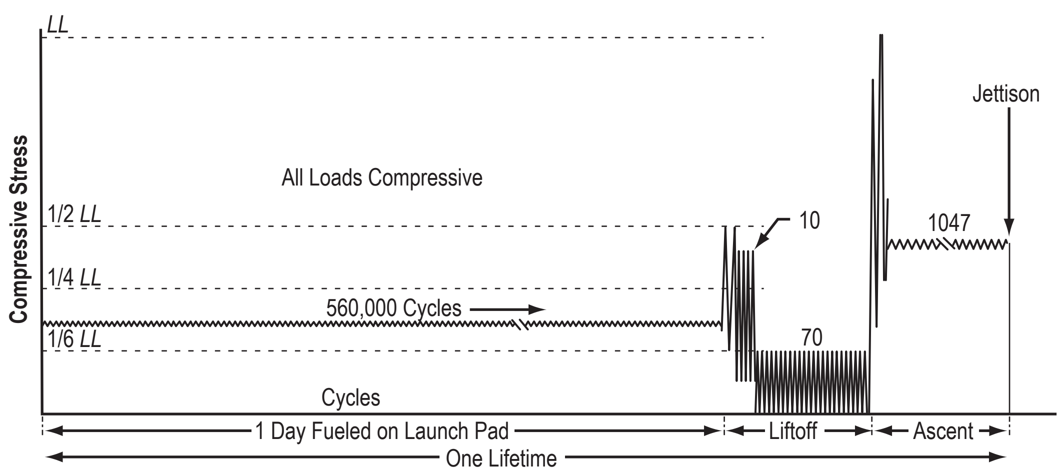

Figure 3. Load spectrum for Ares I interstage.

A launch vehicle structure will typically only experience a few cycles near LL values. Furthermore, it has been demonstrated that detrimental damage growth is not observed at load levels in

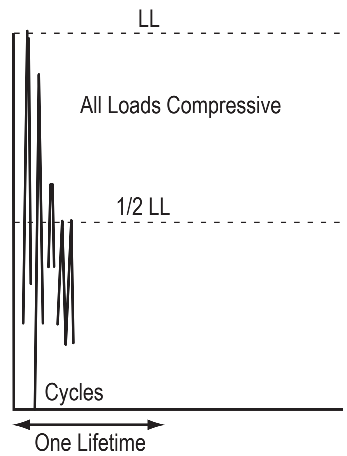

Figure 4. Simplified load spectrum for the Ares I interstage.

a structure designed to accommodate damage. Therefore, it is not necessary to fully develop the curves shown in figure 1 for single-use launch vehicles. By treating the structure as statically loaded, the curves in figure 1 can be greatly simplified.

2.3 Limit Load (Stress) Value in Design and the Need for Compression Fatigue Data

The structural LL is the maximum load that is predicted for the structure to withstand during operating conditions. Design teams use this value, coupled with the material capability, to develop hardware sizing information. Typically, the structural LL is used, along with the required safety factor, to determine the UL for use in design assessments or hardware test programs. The design UL is then compared to the material UL capability as the primary measure for structural capability.

Alternatively, a value for material limit stress (or load) may be developed and used as a direct comparison to the structural limit stress (or load). The material LL is the measure of ultimate strength for the required safety factor and will be designated as σ_{LL} in this TP. For manned spaceflight hardware, the required ultimate factors are 1.4 and 2 for net section and discontinuities, respectively. Ideally, the design is optimized to minimize weight such that the structural limit stress is only slightly lower than the material limit stress.

The material σ_{UL} calculated is usually a 'basis' value at which only 10% of the specimens (B-Basics) are expected to fail. For the composite laminate planned for the acreage of Ares I Upper Stage Interstage, this basis value for CAI loading is ≈86% of the average CAI strength (for any damage severity).[34] Thus, the material limit stress (σ_{LL}) for net section acreage capability in this particular case is calculated by

$$\sigma_{LL} = 0.86/1.4\ (\mathrm{CAI}_{AVG}) = 61.4\%\ \text{of average static CAI strength} \quad . \tag{1}$$

Once the safety factors and basis values are accounted for, the σ_{LL} is 61.4% of the average static CAI strength, and stresses (loads) above this value result in a negative margin of safety. If one accepts the premise that compression fatigue load values <60% of the average static CAI strength are not significant for an impact-damaged laminate,[8,16] then it appears that compression-compression fatigue testing becomes unnecessary. Moreover, reference 10 indicates no damage growth prior to 1 million cycles at constant amplitude compression fatigue loads below 75% of the average CAI static strength. These data are especially relevant for expendable launch vehicles that experience a limited number of fatigue cycles. Exceptions may exist for rotating parts or hardware subjected to high vibratory frequencies resulting in a substantial number of fatigue cycles (>1 million cycles).

While most of the CAI strength data are from tests on coupon-size specimens, the static residual strength has been shown to be insensitive to specimen size and curvature.[35] No observed growth on numerous subscale and two full-scale test articles of the Boeing 777 empennage structure were reported.[36]

3. EXPERIMENTAL

The premise that fatigue testing will reduce to the static case for compression-dominated loads on expendable launch vehicles was examined using a series of tests at NASA Marshall Space Flight Center (MSFC). CAI strength was the property of interest in this study since (1) compression strength values are most affected by impact damage and (2) the hardware in question, an interstage, is a heavily compression-dominated structure.

3.1 Static Testing

A CAI map was generated in a previous study in which static residual strength as a function of various impact parameters was presented.[37] The results showed that damage width, as measured by NDE, and incident energy of impact were two parameters that gave the most reliable residual compression strength data. The correlation between these measures of damage severity and visual damage is ongoing as BVID is a nonquantitative, subjective measurement. BVID must be defined for a given structure. However, this study is only concerned with post impact fatigue behavior that can be presented as a function of static residual strength for any given level of damage. The results from the static strength study are presented in figure 5 for reference purposes.

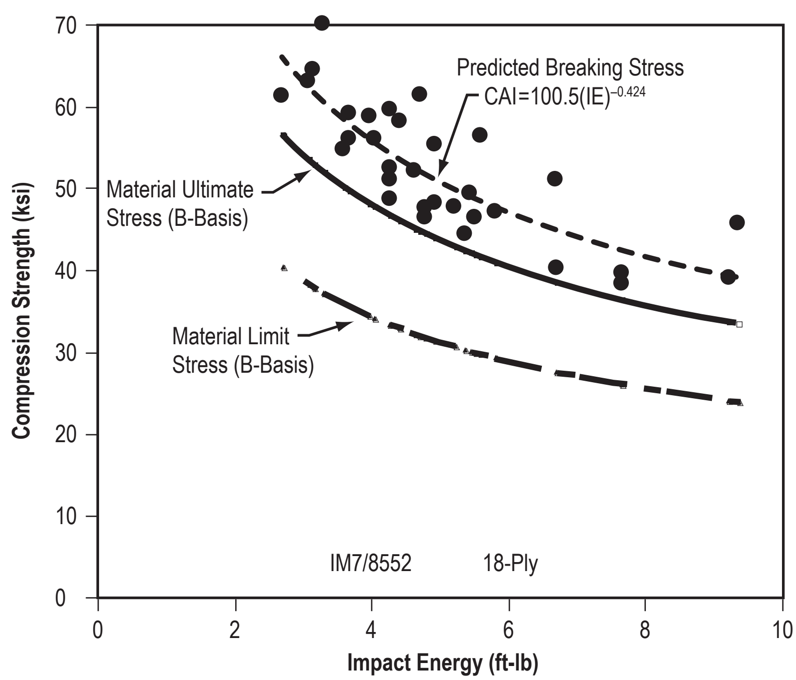

Figure 5. Residual strength (CAI) curve for the Ares I interstage acreage material.

As figure 5 shows, the static compressive load-carrying capability of the sandwich structure drops with increasing impact energy. The testing in this study examined the effects of fatigue on the life of the sandwich panel where the fatigue stress amplitude was measured as a percentage of expected σ_{UL}.

3.2 Cyclic Testing

Constant amplitude cyclic loads were established for a given damage size based on a percentage of B-Basis UL or LL. In this study, the B-Basis load was found to be 86% (A-Basis was 75%) of the expected failure load. Thus, B-Basis UL is 86% of static CAI strength and B-Basis LL is 61% of static CAI strength for any given impact energy. It was decided to test the impact damaged laminates above the B-Basis LL in order to produce a level of conservatism. Since previous work found that a difference of 20% between peak compression amplitudes had no effect on damage size or residual strength,[8] a much larger compression fatigue load difference of 90% was chosen in an attempt to force a change in damage size and residual strength.

3.3 Materials and Specimens

The materials and specimens used in this study were identical to those used for the static testing. They will be briefly reviewed here.

The specimens consisted of composite sandwich panels that were manufactured by a cocure process. The honeycomb core used was perforated 5052 aluminum with a density of 3.1 lb/ft^3 and a thickness of 1.125 in. The face sheets consisted of IM7/8552 carbon/epoxy and the film adhesive used to bond the face sheet to the core was FM 300K with an areal density of 0.08 lb/ft^2. The layup of the face sheet was $(+45,0,–45,0,90,0,0,90,0)_S$.

Each face sheet had a thickness of 0.115 in. The panels were manufactured as 24-×24-in square sandwich plates. All panels were subjected to NDE using infrared thermography (IRT) testing to ensure no flaws were present before specimens were machined from the panels. From the 24-×24-in panels, 4-×6-in specimens were machined for impact and subsequent compression testing. This gave each specimen a cross-sectional area of 0.92 in^2, which was used to calculate the breaking stresses.

After impact, the specimens were inspected with IRT and then were prepared for end loading compression testing. In order to avoid premature failures due to end brooming, the loaded ends of the specimens were potted in an aluminum frame and machined to a tolerance of ±0.001-in parallelism. Details of the specimen geometry are published elsewhere.[34]

3.4 Nondestructive Evaluation Testing

The damage in the specimens was assessed with IRT. IRT is an NDE technique that uses a sensitive infrared camera to monitor heat dissipation from a surface induced with a flash of heat from a quartz lamp. Any areas of damage will dissipate heat at a different rate than undamaged material and the results seen are termed 'indications.' A typical indication for the type of specimen used in this study is shown in figure 6. This two-dimensional indication assesses the planar area of damage with little information about the through thickness characteristics of the damage. Thus, damage growth in this study was measured by any increase in the planar size of the indication.

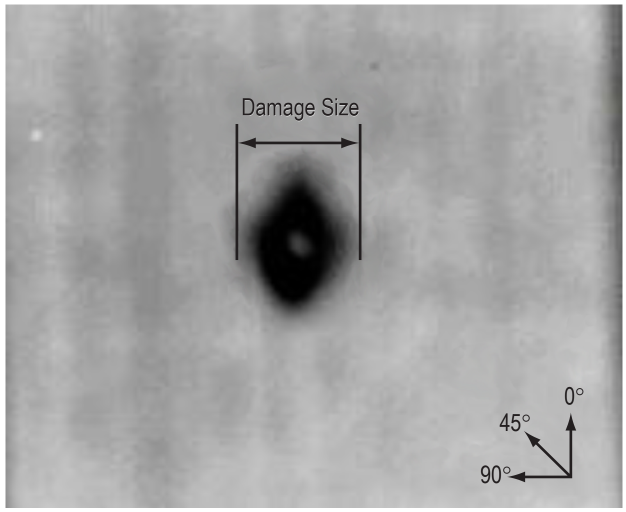

Figure 6. Typical IRT indication of impact-damaged laminate.

4. TEST RESULTS

Testing consisted of the following three phases: (1) Inducing and measuring impact damage size by IRT, (2) fatigue testing and reassessing the damage size, and (3) residual compression strength after fatigue.

4.1 Impact Testing

A total of 30 specimens were impacted at various levels of impact energies for this fatigue study. An impactor with a diameter of 0.5 in was used for all impacts utilizing a drop weight tower that is described in more detail elsewhere.[34] Table 2 presents the impact results of the 30 specimens used for this fatigue study. The solid line in figure 5 represents the expected σ_{UL}.

An example of the visual damage that the specimens incurred is shown in figure 7, where specimens at the low and high ends of impact energies used are presented.

4.2 Fatigue Testing

The maximum compressive fatigue load amplitude was chosen to be more than 100% of the B-Basis LL for a given damage size. For this study, constant amplitude fatigue cycles were applied with the minimum compressive load always set at 10% of the maximum compressive load for an R-ratio equal to 0.1 (a load range of 90%). The loading frequency was 5 Hz. The testing was performed in two series. The first series cycled 15 of the specimens 1,000 times. One thousand cycles is extreme for the Ares I interstage, given that only a few cycles above 50% of LL are expected (fig. 3). If a specimen survived the prescribed 1,000 cycles, it was checked with IRT for damage growth. One thousand additional cycles were applied to the specimen with an additional 10% increase in stress amplitude. After two cyclic stress amplitude increases for a total of 3,000 load cycles, the specimen was tested for static residual compression strength to ascertain any strength degradation due to the severe cyclic loading conditions. The results from the first series of tests are summarized in table 3 for B-Basis σ_{UL} and σ_{LL} and table 4 for A-Basis σ_{UL} and σ_{LL}.

All 15 specimens survived the 3,000 cycles and no growth of the damage area could be detected during any of the three loading phases. Ten percent of the specimens were expected to fail at one cycle when the fatigue stress amplitude was 100% of σ_{UL}, since this is the B-Basis failure stress. Given that the composite interstage structure sees about three load excursions of significance and since the structural LL will be less than or equal to the material LL, no further fatigue testing is necessary to validate the fatigue life of the impact-damaged material of which the composite interstage is comprised. Despite this early observation, this study progressed to even more aggressive fatigue testing to push the limits since the validity of the design envelope can only be demonstrated by testing outside of the envelope.

Table 2. Impact results for specimens to be fatigue tested.

Specimen I.D.	Impact Energy (ft-lb)	Damage Width (in)	Expected Ultimate Stress (ksi)*
F-18-1	2.6	0.44	57.6
F-18-2	3.4	0.45	51.4
F-18-3	3.4	0.49	51.4
F-18-4	3.1	0.56	53.5
F-18-5	3.1	0.49	53.5
F-18-6	4.1	0.56	47.5
F-18-7	4	0.51	48
F-18-8	3.9	0.6	48.5
F-18-9	4	0.56	48
F-18-10	4	0.6	48
F-18-11	9.7	1	33
F-18-12	9.9	0.93	32.7
F-18-13	9.8	0.98	32.8
F-18-14	9.8	0.89	32.8
F-18-15	9.8	0.89	32.8
F2-18-1	3.7	0.71	49.6
F2-18-2	4.4	0.74	46.1
F2-18-3	5.7	0.96	41.3
F2-18-4	7.9	0.93	36
F2-18-5	8.7	0.98	34.5
F2-18-6	8.6	0.92	34.7
F2-18-7	9.8	0.98	32.8
F2-18-8	11.1	0.97	31.1
F2-18-9	11.8	0.94	30.3
F2-18-10	8.1	0.9	35.6
F2-18-11	5.4	0.87	43.3
F2-18-12	6.8	0.89	38.3
F2-18-13	12.2	0.85	29.9
F2-18-14	12.2	0.9	29.9
F2-18-15	12.1	0.74	30

*As determined by reference 37

For 15 additional specimens, the number of fatigue cycles was increased to 10,000. Only one stress amplitude was used since some specimens did fail during the fatigue testing. A summary of these specimens is presented in table 5.

In this series of fatigue tests, 5 of the 15 specimens failed before 10,000 cycles. Two of these failed specimens were at the two highest load amplitudes tested. Damage growth was detected on only two of the surviving specimens; however, the two specimens exhibiting damage growth maintained a residual strength >96% of the expected static strength. The results are plotted in figure 8 to observe trends. The number next to each datum that demonstrated failure is the impact energy in foot-pounds that the specimen was damaged with.

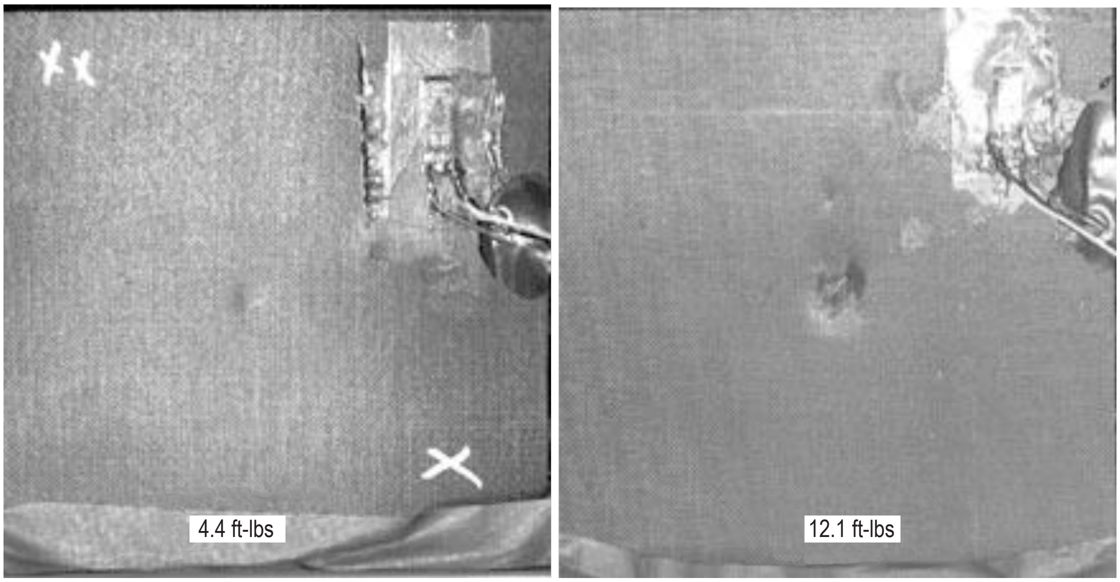

Figure 7 Examples of the visual damage caused by impacts.

Table 3. B-Basis summary of the first series of fatigue after impacts tests: 1,000 cycles per stress amplitude.

Specimen I.D.	First Cyclic Stress Amplitude (ksi)	Percentage of σ_{AVG}/ σ_{BUL}/ σ_{BLL}	Second Cyclic Stress Amplitude (ksi)	Percentage of σ_{AVG}/ σ_{BUL}/ σ_{BLL}	Third Cyclic Stress Amplitude (ksi)	Percentage of σ_{AVG}/ σ_{BUL}/ σ_{BLL}	Percent Growth in Area of Delamination
F-18-1	49.9	75/87/122	54.9	82/95/133	59.9	89/104/146	0
F-18-2	43.6	73/85/119	47.9	80/93/130	52.3	88/102/143	0
F-18-3	45	76/88/123	49.3	84/98/137	54	90/105/147	0
F-18-4	46.5	75/87/122	51.2	83/96/134	55.9	90/105/147	0
F-18-5	42.2	68/79/111	46.4	75/87/122	50.7	82/95/133	0
F-18-6	34.7	63/73/102	38.2	69/80/112	41.6	76/88/123	0
F-18-7	40.9	73/85/119	45	81/94/132	49	88/102/143	0
F-18-8	38.7	69/80/112	42.6	76/88/123	46.4	83/96/134	0
F-18-9	39.8	71/83/116	43.8	78/91/127	47.8	86/100/140	0
F-18-10	39.8	71/83/116	43.8	78/91/127	47.8	86/100/140	0
F-18-11	20.5	53/62/87	22.5	58/68/95	24.6	65/75/105	0
F-18-12	25	65/76/106	27.5	72/84/118	30	79/92/129	0
F-18-13	23.5	66/77/108	28.2	74/86/120	30.7	81/94/132	0
F-18-14	23.5	62/72/101	28.2	74/86/120	30.7	81/94/132	0
F-18-15	25	65/76/106	27.5	72/84/118	30	78/91/127	0

Table 4. A-Basis summary of the first series of fatigue after impacts tests: 1,000 cycles per stress amplitude.

Specimen I.D.	First Cyclic Stress Amplitude (ksi)	Percentage of σ_{AVG}/ σ_{AUL}/σ_{ALL}	Second Cyclic Stress Amplitude (ksi)	Percentage of σ_{AVG}/ σ_{AUL}/σ_{ALL}	Third Cyclic Stress Amplitude (ksi)	Percentage of σ_{AVG}/ σ_{AUL}/σ_{ALL}	Percent Growth in Area of Delamination
F-18-1	49.9	75/100/140	54.9	82/109/153	59.9	89/119/166	0
F-18-2	43.6	73/97/136	47.9	80/107/149	52.3	88/117/164	0
F-18-3	45	76/101/142	49.3	84/112/157	54	90/120/168	0
F-18-4	46.5	75/100/140	51.2	83/111/155	55.9	90/120/168	0
F-18-5	42.2	68/91/127	46.4	75,100/140	50.7	82/109/153	0
F-18-6	34.7	63/84/118	38.2	69/92/129	41.6	76/101/142	0
F-18-7	40.9	73/97/136	45	81/108/151	49	88/117/164	0
F-18-8	38.7	69/92/129	42.6	76/101/142	46.4	83/111/155	0
F-18-9	39.8	71/95/133	43.8	78/104/146	47.8	86/115/161	0
F-18-10	39.8	71/95/133	43.8	78/104/146	47.8	86/115/161	0
F-18-11	20.5	53/71/99	22.5	58/77/108	24.6	65/87/121	0
F-18-12	25	65/87/121	27.5	72/96/134	30	79/105/148	0
F-18-13	23.5	66/88/123	28.2	74/99/138	30.7	81/108/151	0
F-18-14	23.5	62/83/116	28.2	74/99/138	30.7	81/108/151	0
F-18-15	25	65/87/121	27.5	72/117/134	30	78/104/146	0

Table 5. Summary of the second series of fatigue after impacts test.

Specimen I.D.	Max Compressive Stress (ksi)	Percentage of σ_{AVG}/σ_{BUL}/σ_{BLL}	Percentage of σ_{AVG}/σ_{AUL}/σ_{ALL}	Number of Cycles to Failure	Percent Growth in Area of Delamination
F2-18-1	43.1	75/87/122	75/100/140	3,339	N/A
F2-18-2	37.5	70/81/113	70/93/131	9,147	N/A
F2-18-3	27	56/65/91	56/75/105	Survived 10^4	0
F2-18-4	28	67/78/109	67/89/125	Survived 10^4	0
F2-18-5	25.7	64/74/104	64/85/119	Survived 10^4	0
F2-18-6	28.8	71/83/116	71/95/133	Survived 10^4	0
F2-18-7	26.8	71/82/115	71/95/133	Survived 10^4	0
F2-18-8	26.4	73/85/119	73/87/136	Survived 10^4	0
F2-18-9	28.6	81/94/132	81/108/151	Survived 10^4	47
F2-18-10	33.9	82/95/133	82/109/153	8,223	N/A
F2-18-11	35.9	73/85/119	73/97/136	Survived 10^4	0
F2-18-12	34.2	77/89/125	77/103/144	Survived 10^4	0
F2-18-13	29.3	83/98/137	83/111/155	Survived 10^4	93
F2-18-14	29.8	86/100/140	86/115/161	8,312	N/A
F2-18-15	30.9	89/103/144	89/119/166	3,341	N/A

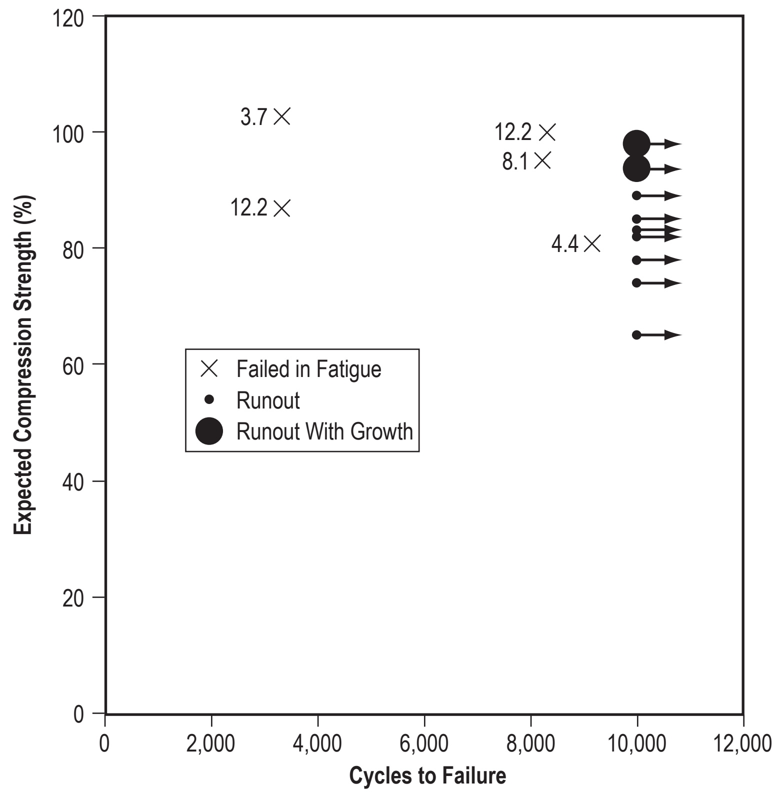

Figure 8. Plot of results from table 5.

From this plot, the only basic conclusion that can be drawn is that, in general, higher fatigue loads are more detrimental. It also appears that the level of impact damage has no effect when the fatigue stresses are based as a percentage of predicted CAI strength. Although the evaluation and quantification of any possible trends would require additional specimens, the number of cycles experienced by expendable launch vehicles is very low with stress amplitudes generally <60% of σ_{UL}.

The IRT results of a typical specimen and the two specimens that exhibit damage growth are shown in figure 9. The dotted oval in each left image is superimposed over the corresponding image on the right to give a qualitative measurement of damage growth.

The IRT technique is not as precise at quantifying damage size as some types of NDE. However, IRT is the most likely candidate for use in the field, so it was employed here.

4.3 Residual Strength Testing

Table 6 shows the results from the static compression strength testing of the specimens in this study that survived the fatigue loading.

The conclusion drawn from this testing is that fatigue tends to increase the compression strength of damaged material. This phenomena has been observed in other studies that examined

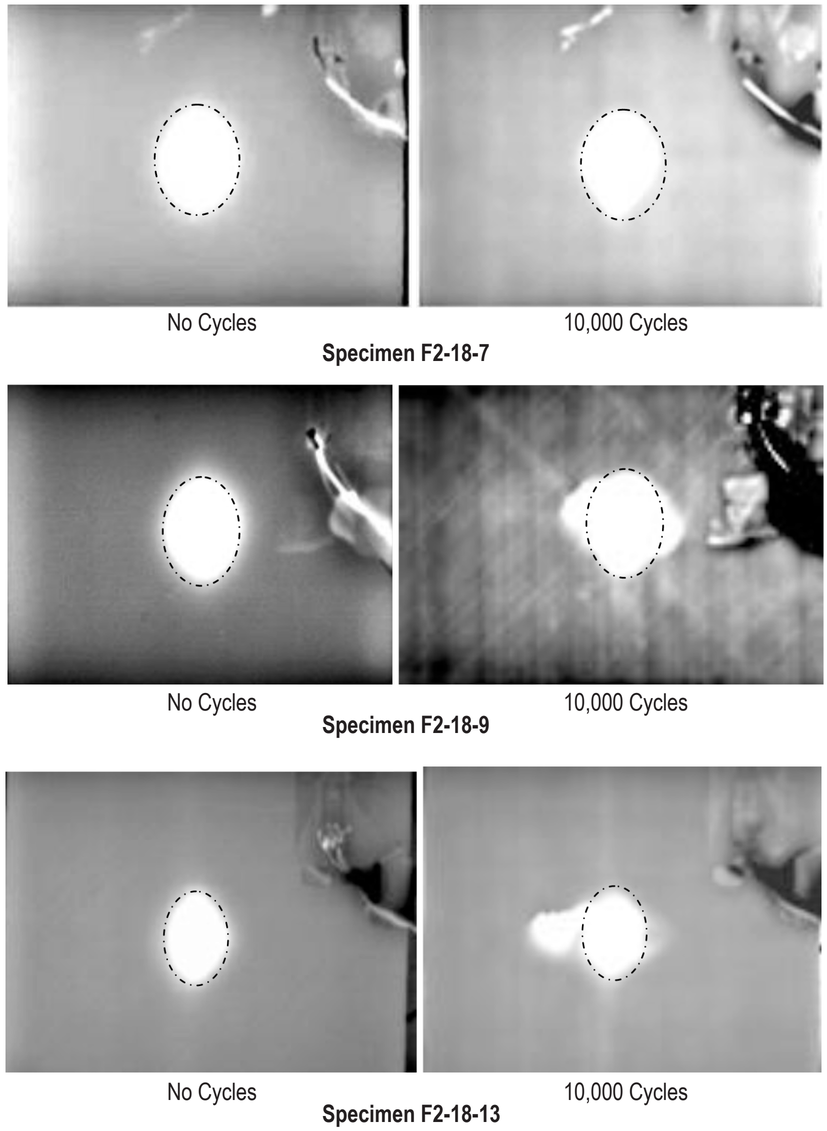

Figure 9. IRT results of a typical specimen (no growth) and the two specimens that exhibit damage growth after 10,000 cycles.

the residual strength of specimens that had survived a fatigue regimen.[2,5,6,8,11,18] Only one reference could be found where fatigue decreased the CAI strength of the laminates.[17] In that reference, the high amplitude loads were held for 120 s, perhaps indicating a creep rupture phenomena that may need to be explored for parts experiencing long dwell times at UL.

Table 6. Static compressive breaking stress of specimens that survived all fatigue series.

Specimen I.D.	Residual Compression Strength (ksi)	Percent of Expected Residual Compression Strength (σ_{AVG})
F-18-1	73.7	111
F-18-2	74.6	115
F-18-3	71.2	116
F-18-4	64.9	117
F-18-5	69.1	113
F-18-6	59.9	108
F-18-7	62.1	105
F-18-8	64.7	122
F-18-9	61.4	110
F-18-10	63	119
F-18-11	49.7	136
F-18-12	49.1	127
F-18-13	48.2	130
F-18-14	38.3	96
F-18-15	46.6	117
F2-18-3	46.8	98
F2-18-4	41.6	100
F2-18-5	38.1	95
F2-18-6	39.5	98
F2-18-7	41.1	108
F2-18-8	38.1	105
F2-18-9*	33.9	96
F2-18-11	45.4	92
F2-18-12	39.5	89
F2-18-13*	36.6	105

*Specimen exhibited damage growth.

5. DISCUSSION

In assessing the damage tolerance approach to human-rated expendable launch vehicles according to reference 1, it is evident that the required coupon-level testing reduces to a static case. The aspects of repeated loading will have no effect on the composite laminate when compressive in-plane loading is involved. Using conservative assumptions, no more than three cycles to LL are expected for the Ares I composite interstage. Thus, the number of fatigue cycles used in this test program where high by at least two orders of magnitude.

All evidence from this and past studies indicate that compression fatigue loading will increase the residual strength of the material. Also, once cyclic loading has ceased to increase the residual compression strength, the residual compression strength reverts back to the static case. Thus, static residual strength is a lower bound for laminates used in expendable load vehicles and development of figure 1(a) is unnecessary.

Figure 1(b) can be simplified since the diagram will consist of data in unrealistic regions of stress amplitude and/or number of cycles to LL as shown schematically in figure 10. Figure 10 combines some of the values given in the references in table 1 with the data in this study. No growth or failures occurred after 10,000 cycles at loads as high as 60% of the expected average failure load, which represents the approximate greatest allowable LL for a given damage size.

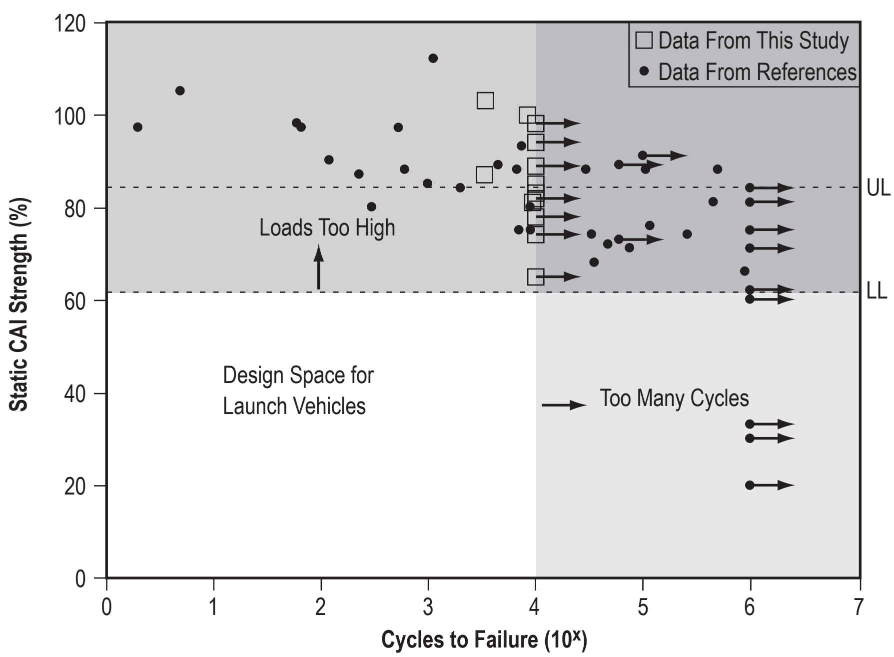

Figure 10. Fatigue life data from this and other studies.

The necessity of constructing figure 1(c) is dubious, as specimens that exhibited damage growth were stronger than equivalent ones that were not fatigued. In addition, detection of damage growth is difficult and has been shown to occur either at the early stages of a specimen's fatigue cycle (which is associated with an increase in strength) or near the end of a specimen's life (when failure is catastrophic), and the number of cycles to failure cannot be predicted with any semblance of accuracy due to the large amount of scatter in the data. Because of the rapid growth at the end of life, the number of cycles to failure is difficult to predict making end-of-life growth measurements difficult. The first two of three phases of fatigue life illustrated in figure 2 were demonstrated in this study. Phase 1 was demonstrated by the 1,000-cycle specimens getting stronger and phase 2 was demonstrated by the 10,000-cycle specimen's strength remaining the same.

6. CONCLUSIONS

From this study, it appears that all fatigue load cases can be considered static for expendable launch vehicles subjected to in-plane compressive loads. The number of cycles is low and the maximum applied stress is just at the level needed for fatigue failure. Tight corners, ramps, and other discontinuities may be affected by fatigue loading but the in-plane CAI properties are not. If a subcomponent or full-scale static test shows out-of-plane failure, then fatigue loading may be of a concern; however, if an out-of-plane failure occurs, the part may need to be redesigned. Thus, fatigue testing is unnecessary above the coupon level.

The data from the experiments in this study corroborate with those from other studies in which a fatigue limit above 60% of CAI strength exists for laminates. In this particular case, since runout was reduced to 10,000 cycles, the fatigue limit was >80% of CAI strength, which should never occur in a launch vehicle structure since structural LL is, at most, equal to the material UL reduced by a safety factor that makes the maximum allowed load about 61% of average CAI strength. Other conclusions from this study include the following:

- Setting a prescribed number of loads and load amplitudes based upon the load spectrum of the component to test fatigue life should take place on a case-by-case basis to provide more flexibility than setting fixed numbers such as presented in reference 1.

- Undamaged specimens have a steeper S-N curve and indicate that specimens that are impact damaged are less affected by fatigue. Thus, any fatigue tests that are warranted should occur on undamaged specimens to obtain a 'worst case' life curve.

- Impact damage growth cannot be used as a clear degradation parameter since most laminates that showed growth had improved or exhibited no change in CAI strengths.

- A full-scale fatigue test is not needed for a composite structure provided that the development and full-scale static tests are successful This same conclusion was reached by those who originally were responsible for developing the load enhancement factor approach for composite laminates.[38]

REFERENCES

1. *NASA Marshall Space Flight Center Fracture Control Requirements for Composite and Bonded Vehicle and Payload Structures*, MSFC–RQMT–3479, Marshall Space Flight Center, AL, June 2006.

2. Rosenfeld, M.S.; and Gause, L.W.: "Compression Fatigue Behavior of Graphite/Epoxy in the Presence of Stress Raisers," *Fatigue of Fibrous Composite Materials, ASTM STP 723*, American Society for Testing and Materials, pp. 174–196, 1981.

3. Ramkumar, R.L.: "Effect of Low-Velocity Impact Damage on the Fatigue Behavior of Graphite/Epoxy Laminates," *Long-Term Behavior of Composites, ASTM STP 813*, T.K. O'Brien (ed.), American Society for Testing and Materials, pp. 116–135, 1983.

4. Griffin, C.F.; and Becht, G.J.: "Fatigue Behavior of Impact Damaged BMI and Thermoplastic Graphite Composites," *Proceedings, 36th International SAMPE Symposium and Exhibition*, San Diego, CA, Part 2, pp. 2197–2209, April 15–18, 1991.

5. Ong, C.-L.; Sheu, M.-F.; Liou, Y.-Y.; and Hsiao, T.-J.: "The Study of the Fatigue Characteristics of Composite After Impact," *Proceedings, 36th International SAMPE Symposium and Exhibition*, San Diego, CA, pp. 912–923, April 15–18, 1991.

6. Krafchak, T.M.; Petra, J.-M.; Davidson, B.D.; and Chen, G.-S.: "Effect of Impact Damage on the Compression Fatigue Behavior of Composite Tubes," *AIAA Paper 93-13999-CP*, *Proceedings, AIAA/ASME/ASCE/AHS/ASC Structures,* Structural Dynamics, and Material Conference, La Jolla, CA, pp. 859–866, April 19–22, 1993.

7. Portanova, M.A.; Poe, C.C.; and Whitcomb, J.D.: "Open Hole and Post-Impact Compression Fatigue of Stitched and Unstitched Carbon/Epoxy Composites," *NASA/TM—1990–102676*, Langley Research Center, Hampton, VA, June 1990.

8. Mitrovic, M.; Hahn, H.T.; Carman, G.P.; and Shyprykevich, P.: "Effect of Loading Parameters on the Fatigue Behavoir of Impact Damaged Composite Laminates," *Comp. Sci. and Tech.*, Vol. 59, pp. 2059–2078, 1999.

9. Symons, D.D.; and Davis, G.: "Fatigue Testing of Impact-Damaged T300/914 Carbon-Fiber-Reinforced Plastic," *Comp. Sci. and Tech.*, Vol. 60, pp. 379–389, 2000.

10. Chen, A.S.; Almond, D.P.; and Harris, B.: "In Situ Monitoring in Real Time of Fatigue-Induced Damage Growth in Composite Materials by Acoustography," *Comp. Sci. and Tech.*, Vol. 61, pp. 2437–2443, 2001.

11. Shyprykevich, P.; Tomblin, J.; Ilcewicz,L.; et al.: "Guidelines for Analysis, Testing and Nondestructive Inspection of Impact-Damaged Composite Sandwich Structures," *DOT/FAA/AR-02/121*, Federal Aviation Administration Technical Center, Atlantic City, NJ, March 2003.

12. Melin, L.G.; and Schon, J.: "Buckling Behaviour and Delamination Growth in Impacted Composite Specimens Under Fatigue Load: An Experimental Study," *Comp. Sci. and Tech.*, Vol. 61, pp. 1841–1852, 2001.

13. Uda, N.; Ono, K.; and Kunoo, K.: "Compression Fatigue Failure of CFRP Laminates With Impact Damage," *Comp. Sci. and Tech.*, Vol. 69, pp. 2308–2314, 2009.

14. Saito, H.; and Kimpara, I.: "Damage Evolution Behavoir of CFRP Laminates Under Post-Impact Fatigue With Water Absorption Environment," *Comp. Sci. and Tech.*, Vol. 69, pp. 847–855, 2009.

15. Gower, M.R.L.; and Shaw, R.M.: "Assessment of the Applicability of Compression-After-Impact (CAI) and Open Hole Tension (OHT) Methods for Use Under Fatigue Loading," *13th European Conference on Composite Materials*, Stockholm, Sweden, June 2–5, 2008, <http://extra.ivf.se/eccm13_programme/program.htm>, Accessed March 3, 2010.

16. Clark, G.; and van Blaricum, T.J.: "Load Spectrum Modification Effects on Fatigue of Impact-Damaged Carbon Fibre Composite Coupons," *Composites*, Vol. 18, No. 3, pp. 243–251, July 1987.

17. Saunders, D.S.; and van Blaricum, T.J.: "Effect of Load Duration on the Fatigue Behavior of Graphite/Epoxy Laminates Containing Delaminations," *Composite.*, Vol. 19, No. 3, pp. 217–228, July 1988.

18. Swanson, S.R.; Cairns, D.S.; Guyll, M.E.; and Johnson, D.: "Compression Fatigue Response for Carbon Fiber With Conventional and Toughened Epoxy Matrices With Damage," *J. Eng. Mater. Technol.*, Vol. 115(1), pp. 116–121, January 1993.

19. Masters, J.E.; and Reifsnider, K.L.: "An Investigation of Cumulative Damage Development in Quasi-Isotropic Graphite/Epoxy Laminates," *Damage in Composite Materials, ASTM STP 775*, K.L. Reifsnider (ed.), American Society for Testing and Materials, pp. 40–62, 1982.

20. Highsmith, A.L.; and Reifsnider, K.L.: "Stiffness-Reduction Mechanisms in Composite Laminates," *Damage in Composite Materials, ASTM STP 775*, K.L. Reifsnider (ed.), American Society for Testing and Materials, pp. 103–117, 1982.

21. Kunz, S.C.; and Beaumont, P.W.R.: "Microcrack Growth in Graphite Fiber-Epoxy Resin Systems During Compressive Fatigue," *Fatigue of Composite Materials, ASTM STP 569*, American Society for Testing and Materials, pp. 71–91, 1975.

22. Han, H.T.; Mitrovic, M.; and Turkgenc, O.: "The Effect of Loading Parameters on Fatigue of Composite Laminates: Part III," *DOT/FAA/AR-99/22*, Federal Aviation Administration, Washington, DC, June 1999.

23. Potter, R.T.: "The Significance of Defects and Damage in Composite Structures," *AGARD Conference on Characterization, Analysis, and Significance of Defects in Composite Materials, AGARD-CP-355*, January 1983.

24. Simonds, R.A.; and Stinchcomb, W.W.: "Response of Notched AS4/PEEK Laminates to Tension/Compression Loading," *Advances in Thermoplastic Matrix Composite Materials, ASTM STP 1044*, G.M. Newaz (ed.), American Society for Testing and Materials, pp. 133–145, 1989.

25. Bakis, C.E.; and Stinchcomb, W.W.: "Response of Thick, Notched Laminates Subject to Tension-Compression Cyclic Loads," *Composite Materials: Fatigue and Fracture, ASTM STP 907*, H.T. Hahn (ed.), American Society for Testing and Materials, pp. 314–334, 1986.

26. Dorey, G.: "Impact and Crashworthiness of Composite Structures," in *Structural Impact and Crashworthiness*, Vol. 1, J. Morton (ed.), G.A.O. Davies (ed.), Elsevier Applied Science Publishers, London, England and New York, New York, pp. 155–192, 1984.

27. Cantwell, W.; Curtis, P.; and Morton, J.: "Post-Impact Fatigue Performance of Carbon Fiber Laminates With Non-Woven and Mixed-Woven Layers," *Composites*, Vol. 14, No. 3, pp. 301–305, 1983.

28. Dorey, G.: "Impact Damage in Composites—Development, Consequences and Prevention," *Proceedings, Sixth International Conference on Composite Materials, Second European Conference on Composite Materials,* E.J. Matthews, N.C.R. Buskell, J.M. Hodgkinson, and J. Morton (eds.), Vol. 3, pp. 3.1–3.26, 1986.

29. Morton, J.; and Godwin, E.W.: "Impact Response of Tough Carbon Fiber Composites," *Comp. Struct.*, Vol. 13. pp. 1–19, 1989.

30. Bishop, S.M.: "The Mechanical Performance and Impact Behavior of Carbon-Fiber Reinforced PEEK," *Comp. Struct.*, Vol. 3, pp. 295–318, 1985.

31. Cantwell, W.J.; Curtis, P.T.; and Morton, J.: "An Assessment of the Impact Performance of CFRP Reinforced With High-Strain Carbon Fibers," *Comp. Sci. and Tech.*, Vol. 25. pp. 133–148, 1986.

32. Puck, A.; and Schurmann, H.: "Failure Analysis of FRP Laminates by Means of Physically Based Phenomenological Models," *Comp. Sci. and Tech.*, Vol. 58, pp. 1045–1067, 1998.

33. Nyman, T.; Ansell, H.; and Blom, A.: "Effects of Truncation and Elimination on Composite Fatigue Life," *Comp. Struct.*, Vol. 48, pp. 275–286, 2000.

34. Nettles, A.T.; and Jackson, J.R.: "Developing a Material Strength Design Value Based on Compression After Impact Damage for the Ares I Composite Interstage," *NASA/TP—2009–215634*, Marshall Space Flight Center, AL, January 2009.

35. Moody, R.C.; Harris, J.S.; and Vizzini, A.J.: "Scaling and Curvature Effects on the Damage Tolerance of Impacted Composite Sandwich Panels," *J. Sand. Struct. Mater.*, Vol. 4, pp. 71–82, 2002.

36. Fawcett, A.; Trostle, J.; and Ward, S.: "777 Empanage Certification Approach," *Proceedings, 11th International Conference on Composite Materials (ICCM-11*), Austrailia, pp. 178–199, July 14–18, 1997.

37. Nettles, A.T.; and Jackson, J.R.: "Compression After Impact Testing of Sandwich Composites for Usage on Expendable Launch Vehicles," *J. Comp. Mater.*, Vol. 44, pp. 707–738, 2010.

38. Whitehead, R.S.; Kan, H.P.; Cordero, R.; and Saether, E.S.: "Cerification Testing Methodology for Composite Structures," DOT/FAA/CT-86/39, Federal Aviation Administration Technical Center, Atlantic City, NJ, October 1986.

REPORT DOCUMENTATION PAGE	*Form Approved* *OMB No. 0704-0188*

1. REPORT DATE *(DD-MM-YYYY)*	**2. REPORT TYPE**	**3. DATES COVERED** *(From - To)*
01–06–2010	Technical Publication	

4. TITLE AND SUBTITLE

Simplification of Fatigue Test Requirements for Damage Tolerance of Composite Interstage Launch Vehicle Hardware

5a. CONTRACT NUMBER

5b. GRANT NUMBER

5c. PROGRAM ELEMENT NUMBER

6. AUTHOR(S)

A.T. Nettles, A.J. Hodge, and J.R. Jackson

5d. PROJECT NUMBER

5e. TASK NUMBER

5f. WORK UNIT NUMBER

7. PERFORMING ORGANIZATION NAME(S) AND ADDRESS(ES)

George C. Marshall Space Flight Center
Marshall Space Flight Center, AL 35812

8. PERFORMING ORGANIZATION REPORT NUMBER

M–1283

9. SPONSORING/MONITORING AGENCY NAME(S) AND ADDRESS(ES)

National Aeronautics and Space Administration
Washington, DC 20546–0001

10. SPONSORING/MONITOR'S ACRONYM(S)

NASA

11. SPONSORING/MONITORING REPORT NUMBER

NASA/TP—2010–216434

12. DISTRIBUTION/AVAILABILITY STATEMENT

Unclassified-Unlimited
Subject Category 24
Availability: NASA CASI (443–757–5802)

13. SUPPLEMENTARY NOTES

Prepared by the Materials and Processes Laboratory, Engineering Directorate

14. ABSTRACT

The issue of fatigue loading of structures composed of composite materials is considered in a requirements document that is currently in place for manned launch vehicles. By taking into account the short life of these parts, coupled with design considerations, it is demonstrated that the necessary coupon level fatigue data collapse to a static case. Data from a literature review of past studies that examined compressive fatigue loading after impact and data generated from this experimental study are presented to support this finding. Damage growth, in the form of infrared thermography, was difficult to detect due to rapid degredation of compressive properties once damage growth initiated. Unrealistically high fatigue amplitudes were needed to fail 5 of 15 specimens before 10,000 cycles were reached. Since a typical vehicle structure, such as the Ares I interstage, only experiences a few cycles near limit load, it is concluded that static compression after impact (CAI) strength data will suffice for most launch vehicle structures.

15. SUBJECT TERMS

composites, damage tolerance, fatigue, requirements, damage growth

16. SECURITY CLASSIFICATION OF: a. REPORT	**b. ABSTRACT**	**c. THIS PAGE**	**17. LIMITATION OF ABSTRACT**	**18. NUMBER OF PAGES**	**19a. NAME OF RESPONSIBLE PERSON**
U	U	U	UU	40	STI Help Desk at email: help@sti.nasa.gov
					19b. TELEPHONE NUMBER *(Include area code)* STI Help Desk at: 443-757-5802

National Aeronautics and
Space Administration
IS20
George C. Marshall Space Flight Center
Marshall Space Flight Center, Alabama
35812